ISOSTATIC STUDIES IN THE HELLENIDES

Chailas,S.*, Hipkin,R.G.** and Lagios,E.*

* Department of Geophysics and Geothermy, University of Athens, Panepistimioupolis, Ilissia, Athens 157 84, GR.
** Department of Geology and Geophysics, University of Edinburgh Mayfield Road, Edinburgh EH9 3JZ, UK.

A B S T R A C T

An isostatic anomaly map, covering Greece, the southernmost part of the Balcan Peninsula, the Aegean and adjacent marine regions, was compiled, based on newly compiled detailed gravity and topographic (2 km grid) data bases, which both extend over a region 900 by 700 km. The 2-dimentional isostatic admittance has been computed for the wavelength range 4 to 900 km. Variation in crustal thickness dominates the long-wavelength admittance contributions so that the part of the gravity field, which is predictable from the topographic load, enables the Moho depth to be mapped. This technique, preliminary results of which are presented in this paper, gives estimates of crustal stretching beta factors which, within the Aegean, reach a maximum in an east-west trending region of the Sea of Crete. The long wavelength parts of the gravity components, which do not correlate with the load, show a simple dipolar anomaly parallel to the Hellenic Trench and characterize the arching and subducting slab. The isostatic admittance appears to be remarkably successful in separating contributions from the slab and crustal thinning. A detailed model of crustal thickness is presented, although the model used may be inappropriate in the fore-arc region. There is no evidence for remnants of former subduction zones.

ΙΣΟΣΤΑΤΙΚΗ ΜΕΛΕΤΗ ΤΩΝ ΕΛΛΗΝΙΔΩΝ ΟΡΟΣΕΙΡΩΝ.

Χαΐλάς,Σ., Hipkin,R.G. και Λάγιος,Ε.

Π Ε Ρ Ι Λ Η Ψ Η

Ενας χάρτης ισοστατικών ανωμαλιών που καλύπτει την Ελλάδα, το νοτιότερο μέρος της Βαλκανικής χερσονήσου, το Αιγαίο και τις γύρω περιοχές έχει δημιουργηθεί με βάση τους πρόσφατα συνταχθέντες λεπτομερείς βαρυτικούς και τοπογραφικούς χάρτες (βήμα 2 km) οι οποίοι καλύπτουν μιά περιοχή 900 επί 700 km. Υπολογίστηκε η δισδιάστατη ισοστατική αντιστάθμιση για μήκη κύματος από 4 ως 900 km. Οι μεταβολές του πάχους του φλοιού κυριαρχούν στη συνεισφορά της αντιστάθμισης μεγάλου μήκους κύματος έτσι ώστε μέρος του βαρυτικού πεδίου, το οποίο μπορεί να υπολογιστεί από την τοπογραφική φόρτιση, επιτρέπει την χαρτογράφηση του βάθους της Moho. Αυτή η τεχνική, αρχικά

αποτελέσματα της οποίας παρουσιάζονται σ' αυτή την εργασία, επιτρέπει τον υπολογισμό του συντελεστή εφελκυσμού b για την περιοχή του Αιγαίου ο οποίος παίρνει τη μέγιστη του τιμή στην Ανατολικής-Δυτικής διεύθυνσης θάλασσα της Κρήτης. Οι μεγάλου μήκους κύματος ανωμαλίες του βαρυτικού πεδίου που δεν συσχετίζονται με το φορτίο δείχνουν μία διπολική ανωμαλία παράλληλα με την Ελληνική τάφρο που χαρακτηρίζει την εξωτερική και βυθιζόμενη πλάκα. Η ισοστατική συνάρτηση μεταφοράς φαίνεται ότι είναι ιδιαίτερα επιτυχής στη διάκριση της συνεισφοράς της βύθισης και της λέπτυνσης του φλοιού. Ενα λεπτομερές μοντέλο του πάχους του φλοιού παρουσιάζεται παρόλο που πιθανόν να είναι ανακριβές για την περιοχή εξωτερικά του τόξου. Δεν υπάρχουν ενδείξεις για υπολείμματα παλαιών ζωνών κατάδυσης.

INTRODUCTION

The original studies of isostasy, for example by Hayford (1912), Heiskanen (1924) and Vening-Meinesz (1931), started with a specific mechanism of isostasy and then corrected gravity data for its effects. In recent work (Dorman and Lewis, 1970, Lewis and Dorman, 1970), an intermediate stage has been introduced, where a relation between the applied load and the resulting gravity anomaly is determined first. This relation, represented by the isostatic response function, is objective and not particular to only one specific mechanism. The response function can be then modelled in order to find a best-fitting compensation process. The present paper describes an investigation of isostasy in the area of Greece, using a new compilation of gravity and topographic data.

THEORY

Isostatic Admittance

The Bouguer anomaly, Δg, can be considered as the sum of two parts (Dorman and Lewis ,1970): first, the contribution from masses involved in the compensation and, secondly, the contribution from uncompensated variations in density, Δg_ρ. The first part is predictable from the topographic load, h, and, in the linear approximation, is obtained by convolving the topographic load with the isostatic response of the Earth to a point load, a relation expressed as:

$$\Delta g = g * h + \Delta g_\rho \qquad (1)$$

where the operator * denotes convolution, q is the isostatic response function and the term Δg_ρ expresses a function of non-isostatic density distribution.

In fact, the quantity q*h is not representing the gravity contribution from the compensation of the topographic load. It describes the statistical relation between the topography and the gravity contribution from all masses involved in compensation (topography included). The isostatic response function in (1) can be treated mathematically as the space domain transform of the result of the normalization in the wavenumber domain of the

gravity by the respective topography. All the information about the isostatical regime of area under consideration is included in the isostatic response function.

In the wavenumber domain, the relation (1) becomes:

$$G(k) = Q(k)\,H(k) + N_G(k) \qquad (2)$$

G(k), H(k) and $N_G(k)$ are the 2D Fourier transforms of the Bouguer gravity anomaly, the topography and the part of the gravity anomaly, which is generated by uncompensated masses. The isostatic admittance, Q(k), is the Fourier transform of the isostatic response function, estimated from:

$$Q(k) = \frac{\langle G(k)\,H^*(k)\rangle}{\langle H(k)\,H^*(k)\rangle} - \frac{\langle N_G(k)\,H^*(k)\rangle}{\langle H(k)\,H^*(k)\rangle} \qquad (3)$$

where the asterisk denotes the complex conjugate (see McKenzie and Bowin, 1976). Because Δg_o and h are defined to be uncorrelated, the contribution of the second term in equation (3) will be diminished when the spectral estimates are averaged and, ultimately, will become zero. The averaging process, denoted in equation (3) by the triangular brackets, takes the mean around concentric annuli in the wavenumber domain, that is, it averages the estimates whose wavenumber has a similar magnitude, independently of the direction of their trend. We use wavenumber intervals, which are logarithmically spaced, in order to get approximately equal numbers of estimates in each wavenumber band.

The fraction of the total gravity variance at wavenumber k that can be attributed to the linear isostatic relation is given by the coherence:

$$\gamma^2_{GH}(k) = \frac{\langle Q(k)\,H^*(k)\rangle\ \langle G^*(k)\,H(k)\rangle}{\langle G(k)\,G^*(k)\rangle\ \langle H(k)\,H^*(k)\rangle} \qquad (4)$$

The Isostatic Compensation Model

The gravitational attraction of an interface of contrasting density, which undulates with an amplitude w(x) from its mean depth d, was given by Parker (1972). When w(x) << d, it simplifies to a linear relation, which can be given in the wave number domain as:

$$G(k) = 2\pi\gamma\,(\Delta\rho)\,e^{-kd}\,W(k) \qquad (5)$$

where W(k) is the Fourier transform of w(x) and $\Delta\rho$ is the density contrast at the interface. In general, the undulations of the interface of contrasting density where compensation takes place are related to the topographical load, h(x), by

$$W(k) = K(k)\ H(k) \qquad (6)$$

where K(k) may depend upon the elastic parameters, density contrasts and dimensions involved. By substituting W(k) into equation (5), we have:

$$G(k) = 2\pi\gamma(\Delta\rho)\, e^{-kd} K(k) H(k) \qquad (7)$$

If equation (7) is substituted into equation (3) and the logarithm taken, then

$$\ln(Q(k)) = \ln(2\pi\gamma\Delta\rho) + \ln(K(k)) - kd \qquad (8)$$

For local compensation, K is a constant and, in the simplest case of Airy isostasy, K = 1; then equation (8) becomes :

$$\ln(Q(k)) = \ln(2\pi\gamma\Delta\rho) - kd_H \qquad (9)$$

where it is assumed that d_H is the mean Moho depth. Having found a linear relation, we have used this relation to model the observed isostatic response values.

The determination of the response function as an intermediate stage for the calculation of isostatic correction, gives the advantage of an objective choice of the isostatic model. In other words it gives the ability for the determination of the isostatic regime of the area by the use of objective criteria, such as best fitting.

DATA SOURCES

Topography

On land, the topographic databank was compiled from the maps of the Hellenic Military Geographical Service (HMGS); for the sea, maps of the Hydrographic Service (HS) of the Hellenic Navy and those of Morelli et al. (1975a,b) were used. Mean heights on a 2 km grid were estimated directly from land maps of 1:50,000 with an estimated accuracy of approximately ±10m. Off-shore, depth points of the HS 1:250,000 and 1:500,000 scale maps as well as contours from Morelli's maps (scale 1:1,000,000) were digitised. All data locations were then transformed to UTM zone 34 coordinates and interpolated on to a regular 2 km grid, giving a 350 by 450 array, which represents a low-pass filtered version of the topographic relief in Greece and its neighbourhood.

Gravity

A corresponding 2 km array of gridded Bouguer gravity anomaly values was produced, based on a databank of some 22000 point gravity values, which was previously prepared by Lagios et al. (1988) for the Institute of Geology and Mining Exploration (IGME), Athens, Greece. This databank was itself constructed by verifying and purging data compiled by Makris and Stavrou (1984), again for the IGME, and by adding substantial quantities of previously unpublished IGME data. The compilation covers a great part of the region lying between latitudes 32° and 42°N, and longitudes 19° and 27°E. On the mainland of Greece, data consist of real observations. Off-shore, data were derived by digitising the position where ship tracks crossed contour lines on the gravity maps published by Morelli et al. (1975a,b).

All gravity anomaly values are referred to the IGSN71 (Morelli et al., 1974) and the GRS67 (International Association

of Geodesy, 1971), and reduced with a standard Bouguer density of 2.67 Mg/m3.

In order to provide a complete array within a rectangular area, further data were added along the margins. Along part of the northern margin, contours from an unpublished gravity map of Albania (S. Bushati, personal commun., 1991) were digitised. Elsewhere along this margin, values for the free-air anomaly were calculated using the OSU86E gravity model (Rapp and Cruz, 1986) and then Bouguer anomalies simulated using a digital terrain model to compute the topographic effect. This applied only to a small data gap in southern Yugoslavia and Bulgaria and was designed to minimise edge effects in a more objective way than reflection or ramping. The area of data generated in this way was so small that the use of a specific isostatic model in predicting Bouguer anomalies could not bias our overall interpretation.

Error estimates of the gravity anomalies onland, depending on the way of the height determination of the stations, range from 0,3- 0,9 mGal (Lagios et al,1988)

RESULTS

The Isostatic Admittance

The isostatic admittance was estimated for wavelengths between 4 and 900 km. This range was divided into 1000 intervals, spaced logarithmically so that each contained approximately equal numbers of estimates. Within each wavenumber band, the estimates were averaged in order to reduce the contribution from gravity anomalies not correlated with the topographic load (see equat.3).

Figure 1 shows the resulting isostatic admittance for the Hellenides, with the natural logarithm of the admittance (ln(Q)) plotted against wavenumber for the range of wavelengths from about 80 to 900 km. The linearity shown in this figure is central to our interpretation: it demonstrates that ln(Q) depends very weakly,if at all, on wavenumber, a result indicative of simple local isostatic balance, for example by the Airy model, or equivalently, by an elastic plate with a negligibly small rigidity. In the latter case, internal and surface loading are not distinguishable.

A least-squares fit to the admittance data, weighting each estimate with the inverse of its variance, gives the relation:

$$\ln(Q) = -(2.522 \pm 0.014) - (24.7 \pm 5.5)\,k \quad (km^{-1}) \qquad (10)$$

With the Airy model, the observed slope implies that the mean Moho depth averaged over the land and marine area of the region is 24.7 km. The observed intercept of -2.522 (to be compared with $\ln(2\pi\gamma(\Delta\rho))=-2.179$) indicates that K=0.71; that is 71% of the topographic load is compensated by undulations on the Moho; the remainder is balanced by other mechanisms and seems to be distributed laterally in such a way that it does not correlate with Moho topography.

Once a satisfactory model for the isostatic admittance has been identified (as can be seen by the error estimates of the parameters in equation (10)), and shown to be compatible with a

simple Airy mechanism, it provides a means of isolating the component of the Bouguer anomaly, $\Delta g_{\Delta h}$, which is generated by variations (Δh) in crustal thickness:

$$\Delta g_{\Delta h} = q * h \qquad (11)$$

Here, q is found from the model described by equation (10). Although now an empirical figure of $\Delta g_{\Delta h}$ has been obtained by the gravity observations, this component corresponds with the classical isostatic correction. The remaining part (Δg_{ρ} of equation 1) would classically be known as the isostatic anomaly. This empirical version of the isostatic anomaly will include every density source, whether deeper and shallower than the Moho and whether or not it is isostatically balanced, provided that it is uncorrelated with Moho undulations. For the Hellenides, the isostatic anomaly is probably dominated by the gravity effect of the subducting slab and will be discussed further down.

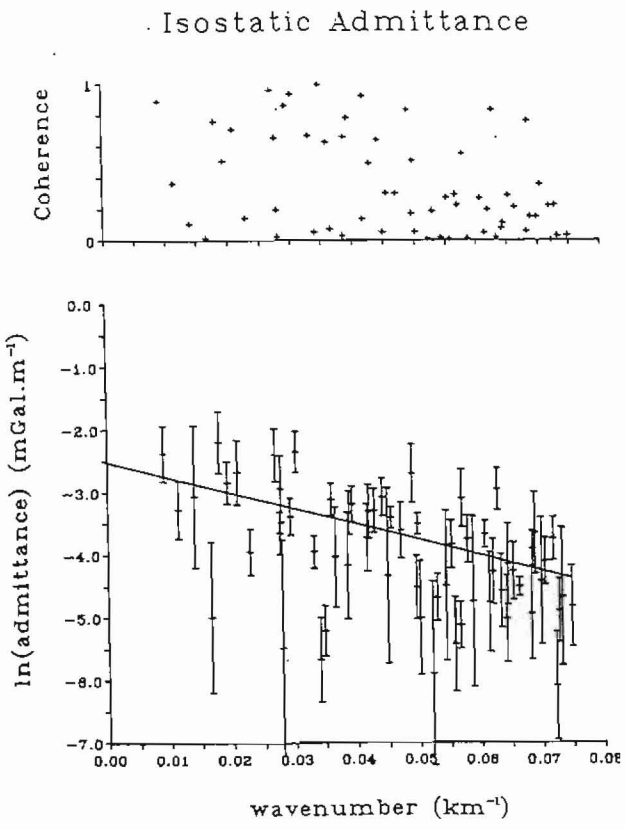

Fig.1. Isostatic Admittance plotted against wavenumber, with corresponding coherence values.

Crustal Thickness Models and the Isostatic Correction.

The average Moho depth of 25 km determined from the isostatic admittance spectrum is satisfactorily consistent with the limited amount of seismic refraction data in the area: in the summary by Makris (1984), most profiles show Moho depths between 20- 30 km, with a local feature under the Peloponnese depressed to 42 km.

Makris (1984) used his compilation of Bouguer anomaly data over the Hellenides to extrapolate the Moho depth from seismic profiles to the whole area. The difficulty with this approach lies in the probability that a large component of the observed Bouguer anomaly is due to the subducted slab, rather than variations in crustal thickness. Using the whole of the Bouguer anomaly for the extrapolation will give too much thinning of the crust over the subducting slab and too large a thickness over the fore-arc bulge. Because the subducting slab component is removed, using the empirical isostatic correction, this provides a more discriminating prediction of crustal thickness than Makris' approach using the whole Bouguer anomaly.

According to the computational procedure, which was implemented, in order to model variations in crustal thickness from the isostatic correction (Fig. 2), two constraining parameters are needed: (i) The density contrast on the Moho and (ii) The Moho depth at one point.

The observational constraints available are the local Moho depth from the seismic profiles and the mean Moho depth over the whole area derived from the admittance spectrum. Matching the available constraints with those required theoretically was done iteratively. Although a more complete search has yet to be completed, the initial results suggest that the density contrast on the Moho is closer to -0.35 Mg/m3 than the conventional value of about -0.5 Mg/m3. Figure 3 shows one inversion of the isostatic correction data to produce Moho depth values.

On land, the greatest thickness occurs under the Peloponnese, reaching 38km, where Makris' refraction data show a local depression of 42km. Because the upward continuation operator attenuates the gravity effect of short wavelength features of Moho topography and the Moho depth map is correspondingly smoothed, the agreement between the abrupt step down to 42km for a 50 km length of one seismic refraction profile and our smooth descent to 38 km is probably as good as can be expected.

Within the Aegean, there are two main regions of enhanced crustal thinning. In the Sea of Crete, there is a region where the b- factor (McKenzie, 1978) reaches 1.32, assuming a normal crustal thickness of 33km. Unlike the corresponding region predicted from the whole Bouguer anomaly, which is more diffuse and arcuate and trends parallel to the trench, our results indicate a somewhat narrower feature, confined to a linear, east-west trending region, parallel to the north coast of Crete. A much less pronounced feature sweeps north from the western end of the Sea of Crete, to the W of Milos, and then NW into the Gulf of Corinth, suggestive of an incipient rift of the Peloponnese away from the remainder of the Hellenic mainland. Most of the rest of the Aegean has relatively small b-factors, between 1.1 and 1.2. The exception is the Northern Aegean Trough, where the

b-factor reaches 1.32.

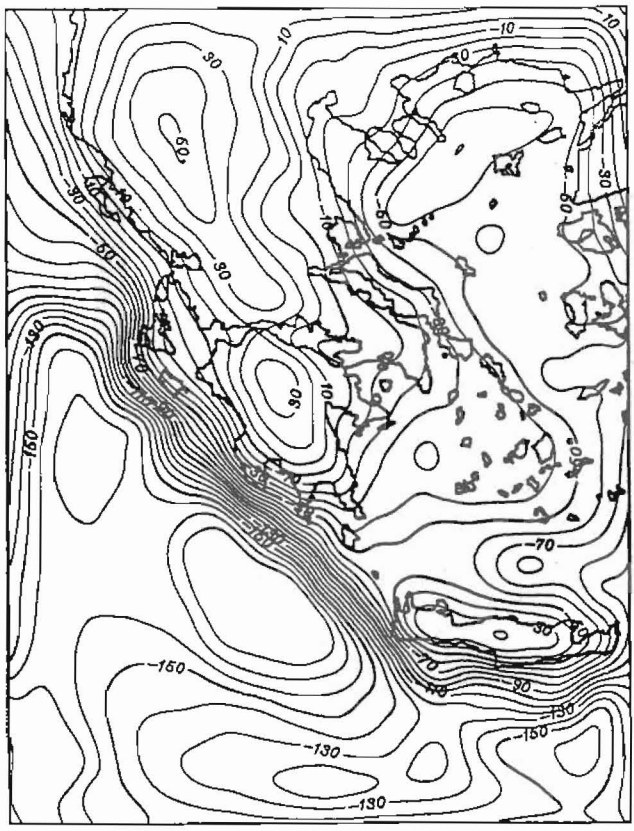

Fig.2. Isostatic Correction Map (in mGals). Frame coordinates are bounded by UTM Zone 34, Eastings 300-1000 km, Northings 4200-5100 km.

While the model (fig. 3) has quantified Moho features within the Aegean in a way which, although more refined, was more or less expected, our apparent prediction of very significantly thinned crust in the fore-arc region was not. The model ostensibly gives b-factors as large as 2.8, close to the limit of oceanic crust, in the fore-arc region of the Mediterranean, between the western end of Crete and south-west of Peloponnese. Although J.E. Dixon (personal commun. 1992) has independently predicted (on the basis of geological aspects) thinned crust in the fore-arc region, having pointed out that the existence of a subducted slab extending under the Aegean to depths of more than 200km requires a greater length of crust to be created than can be provided by the stretching event in the Sea of Crete. For this reason, the results of our analysis may need to be treated with some caution.

According to the analysis presented in this work, the observed gravity observations lead to the estimation of the admittance and, subsequently, to the variation of the Moho depth by the determination of the corresponding gravity anomaly component, provided that a simple Airy mechanism exists. In the tectonic, therefore, regime of the Aegean, where we also have the descending lithospheric plate to the north-east, the density sources within the slab are mostly well separated in depth from those on the Moho. Moreover, the asthenospheric layer, intervening between the descending slab and the over-riding plate, will reduce stress transmission between the two.

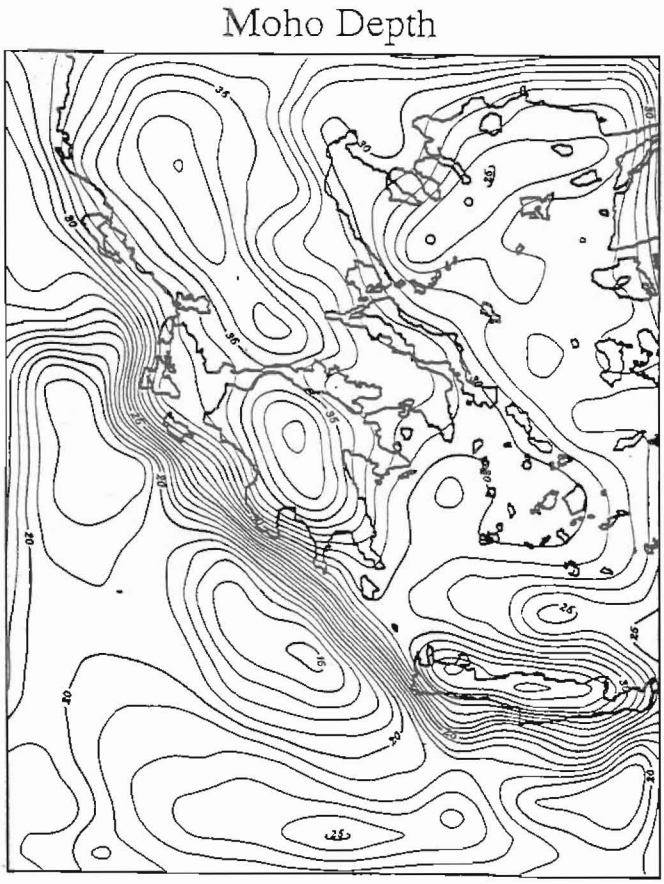

Fig.3. Map showing the variation of Moho depth (in km). Frame is bounded by UTM Zone 34, Eastings 300-1000 km, Northings 4200-5100 km.

In contrast, within the fore-arc region, undulations in Moho-depth are likely to be correlated with undulations in the lithosphere- asthenosphere boundary. It is reminded that the linearity of ln(Q) shown earlier (Fig. 1), indicates either a

simple local isostatic balance (ie. Airy model in the back-arc region) or, equivalently, the presence of an elastic plate (with small rigidity) mechanism, where, however, in the latter case, the internal and surface loading cannot be distinguished. As a consequence, a successful application of a "regionalized" analysis depends mainly on the type of compensational mechanism, which is actually prevailing in an area. In the fore-arc region, a different geotectonic regime exists compared to the back-arc region.

Consequently, an upwarping of the lithospheric plate within the fore-arc bulge will make both the sea bed and the Moho shallower, just as the downwarping, which causes the trench results in a deeper Moho. In such an environment, the tectonic forces generate an admittance contribution with the opposite sign from that required for isostatic balance.If such stress transmission associated with the subducting plate is dominant, using equation (10) to predict the Moho depth, will produce an undulation, which also has the wrong sign. Modelling the Moho depth from the isostatic correction in the fore-arc may then be inappropriate; in this region, modelling may need to involve both the isostatic correction and the isostatic anomaly, because both are generated by the same source. This approach corresponds to Makris' (1984), who used the whole Bouguer anomaly to predict the Moho depth.

The Isostatic Anomaly and Subducting Lithosphere.

The classical technique of regional-residual separation forms an essential, though non-unique, part of gravity interpretation. The separation of the total Bouguer anomaly into isostatic correction and isostatic anomaly should be seen as an objective version of this process. An important and legitimising aspect of gravity interpretation must be that both the residual and the regional anomaly are modelled, so that the sum of the two components generates the total observed gravity field. In the previous section, we proposed that the isostatic correction reflects variations in crustal thickness, at least in the Aegean. Here, we identify the isostatic anomaly with the contribution of the descending lithospheric slab.

The isostatic anomaly map of the area, deduced from the gravity and topographic data banks and the analysis presented above was therefore compiled. The significance of some local features and detailed accounts associated with this map will not be given here. However, a smoother version of this map will be considered in the following, presented in figure 4. This version was produced from the original map by the application of a low-pass filter,(roll-off of 200-250km wavelength) generated to clarify the contribution from the descending slab. The positive feature over the southern Aegean has a simple structure (consistent with a deep source), and is delimited rather precisely by the arc of the Hellenic Trench to the south-west and the volcanic arc to the north-east, and has the expected asymmetry of a feature dipping to the north-east.

We therefore conclude that the technique applied in this work has proved remarkably successful in isolating the gravity effect of the descending lithospheric slab, a task previously confused by the superposition of the similarly positive anomaly,

due to the crustal thinning in the Sea of Crete.

Detailed modelling is as yet incomplete, but the half width of about 100km is consistent with a depth to the top of the source of about 70km (section 2.7.5, Telford et al., 1990), reasonably consistent with the typical thickness of normal lithosphere, below which the descending slab starts to contribute to the gravity anomaly. The anomaly of a dipping slab is not very sensitive to the maximum depth of penetration and, without more detailed modelling, it is premature to attempt to discriminate between a maximum depth of about 200km suggested by the earthquake hypocentral locations (Papazachos and Comninakis, 1971; Papazachos, 1990) or the larger depths, 400 to 600km, suggested by seismic tomography (Spakman et al., 1988). However, the failure of the anomaly to extend much to the north-east of the volcanic arc favours either the former depth range or an increase in dip beyond the deepest earthquakes.

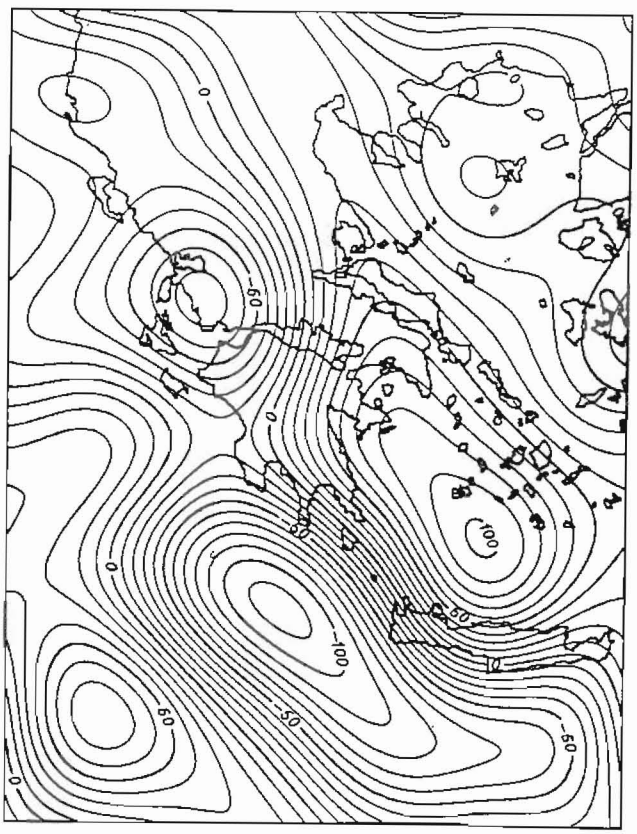

Fig.4. Smoothed version of the Isostatic Anomaly Map (in mGals). Frame is bounded by UTM Zone 34, Eastings 300-1000 km, Northings 4200-5100 km.

A negative but very informative characteristic of the unfiltered isostatic anomaly map is that it is otherwise more or less featureless over the whole area behind the Hellenic Arc. There are no other slab-originated-like anomalies to indicate sub-crustal remnants of former subduction zones associated with the ophiolite sequences in northern Greece. Nor are there significant features on the isostatic anomaly or isostatic correction maps associated with the Meso-Hellenic Trough, or other basins on or off-shore, with the exception of the isostatic anomaly near the Gulf of Patras.

ACKNOWLEDGMENTS

Most of this work was supported by EC Science Program (EEC SCI-492). Mr Stelios Chailas is also thankful to the Hellenic State Studentship Foundation.

REFERENCES

Dorman,L.M. and Lewis,B.T.R., 1970. Experimental Isostasy 1. Theory of the Determination of the Earth's Isostatic Responce to a Concentrated Load. J.Geophys.Res. 75(17), pp.3357-3365.

Hayford,J.F. and Bowie,W., 1912. The effect of topography and isostatic compensation upon the intensity of gravity. US Coast. and Geod. Surv., Spec. Publ. 10, Washington.

Heiskanen,W., 1924. Untersuchungen uber Schwehrkraft und Isostasie. Veroff. Finn. Geod. Inst. 4, Helsinki.

Lagios,E., Hipkin,R.G., Angelopoulos,A. and Nikolaou,S., 1988. The Gravity Anomaly Map of Greece-A Recompilation. Institt. of Geol. and Min. Expl. (IGME), Athens, Greece (in press).

Lewis,B.T.R. and Dorman,L.M., 1970. Experimental Isostasy 2. Anisostatic model for the USA derived from gravity and topographic data. J. Geophys. Res. 75(17), pp.3367-3385.

Makris,J., 1984. Geophysics and geodynamic implications for the evolution of the Hellenides. In: D.J. Stanley and F.C Wezel (editors), Geological evolution of the Mediterranean Basin, Springer-Verlag, New York, pp.231-248.

Makris,J. and Stavrou,A., 1984. Compilation of Gravity Maps of Greece. Techn. Report, Institute of Geology and Mining Exploration, Athens, Greece.

McKenzie,D. and Bowin,C., 1976. The relation between bathymetry and gravity in the Atlantic Ocean. J.Geoph. Res., 81:1903-1915.

McKenzie,D., 1976. Some remarks on the development of sedimentary basins., Earth and Plan. Sc. Letters, 40, 25-32

Vening-Meinesz,F., 1931. Une nouvelle methode pour la reduction isostatique de l'intensite de la pesanteur. Bull. Geod., 29: 33-45.

Morelli,C., Gantar,C., Honkasalo,T., McConnell,R.K., Tanner,J.G., Szabo,B., Uotila,U. and Whaln,C.T., 1974. The International Gravity Standardization Net 1971 (IGSN'71). Spec. Publ. No 4, International Association of Geodesy, Paris.

Morelli,C., Gantar,G., Pisani,M., 1975a. Bathymetry, gravity and

magnetism in the strait of Sicily and in the Ionian sea. Boll. Geofis. Teor. Appl., 17: 39-58.
Morelli,C., Pisani,M., Gantar,G., 1975b. Geophysical Studies in the Aegean Sea and in the Eastern Mediterranean. Boll. Geofis. Teor. Appl., 18: 127-167.
Papazachos,B.C., 1990. Seismicity of the Aegean and surrounding areas. Tectonophysics, 178: 287- 308.
Papazachos,B.C. and Comninakis,P., 1971. Geophysical and tectonic features of the Aegean Arc. J. Geophys. Res., 76, 8517-8533.
Parker,P.L., 1972. The rapid calculation of potential anomalies. Geophys. J. R. astr. Soc., 31: 447-455.
Rapp,R.H. and Cruz,J.Y., 1986. Spherical harmonic expansion of the Earth's gravitational potential to degree 360 using 30' mean anomalies. Rept. No 376, Dept. Geod. Sci. Surv., Ohio State Univ., Columbus.
Spakman,W., Wortel,M.J.R. and Vlaar,N.J., 1988. The Hellenic Subduction Zone: a tomographic image and its geodynamic implications, Geoph. Res. Lett., 15, 60-63.
Telford,W.M., Geldart,L.P. and Sheriff,R.E., 1990. Applied Geophysics, Cambridge Univ. Press, Cambridge.